Konya Mühendislik Bilimleri Dergisi, c. 13, s. 2, 607-623, 2025
Konya Journal of Engineering Sciences, v. 13, n. 2, 607-623, 2025
ISSN: 2667-8055 (Electronic)
DOI: 10.36306/konjes.1649691

DEVELOPMENT OF A TERNARY LEVELS EMOTION CLASSIFICATION MODEL UTILIZING ELECTROENCEPHALOGRAPHY DATA SET

[1,*] Hatice OKUMUS, [2] Ebru ERGUN

[1] *Karadeniz Technical University, Electrical and Electronics Engineering Department, Trabzon, TÜRKİYE*
[2] *Recep Tayyip Erdogan University, Electrical and Electronics Engineering Department, Rize, TÜRKİYE*
[1] haticeokumus@ktu.edu.tr, [2] ebru.yavuz@erdogan.edu.tr

Highlights

- This study segments EEG data and extracts features via Hilbert transform for classification.
- Feed-forward neural networks classify valence and arousal levels with high accuracy.
- EEG feature sets achieve 99.70% arousal and 98.60% valence accuracy in emotion recognition.

Graphical Abstract

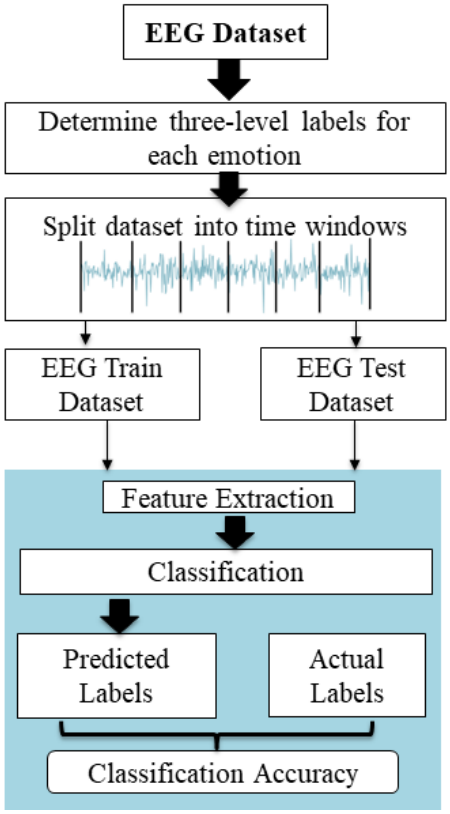

Flowchart of the proposed method

***Corresponding Author:** Hatice OKUMUS, haticeokumus@ktu.edu.tr

Konya Mühendislik Bilimleri Dergisi, c. 13, s. 2, 607-623, 2025
Konya Journal of Engineering Sciences, v. 13, n. 2, 607-623, 2025
ISSN: 2667-8055 (Electronic)
DOI: 10.36306/konjes.1649691

DEVELOPMENT OF A TERNARY LEVELS EMOTION CLASSIFICATION MODEL UTILIZING ELECTROENCEPHALOGRAPHY DATA SET

[1,*] Hatice OKUMUS, [2] Ebru ERGUN

[1] *Karadeniz Technical University, Electrical and Electronics Engineering Department, Trabzon, TÜRKİYE*
[2] *Recep Tayyip Erdogan University, Electrical and Electronics Engineering Department, Rize, TÜRKİYE*
[1] haticeokumus@ktu.edu.tr, [2] ebru.yavuz@erdogan.edu.tr

(Received: 02.03.2025; Accepted in Revised Form: 23.05.2025)

ABSTRACT: Electroencephalogram (EEG)-based emotion recognition has gained increasing attention due to its potential in objectively assessing affective states. However, many existing studies rely on limited datasets and focus on binary classification or narrow feature sets, limiting the granularity and generalizability of their findings. To address these challenges, this study explores a ternary classification framework for both valence and arousal dimensions—dividing each into low, medium, and high levels—to capture a broader spectrum of emotional responses. EEG recordings from ten randomly selected participants in the DEAP dataset were used. Each 60-second EEG segment was divided into six non-overlapping windows of 10 seconds to preserve temporal stability and extract reliable features. The Hilbert Transform was applied to compute instantaneous amplitude and phase information, enabling the detection of subtle variations in emotional states. These features were then classified using a feed-forward neural network. The proposed approach achieved impressive classification accuracies of 99.13% for arousal and 99.50% for valence, demonstrating its effectiveness in recognizing multi-level emotional states. By moving beyond binary labels and leveraging time-frequency domain features, this study contributes to the development of more refined and responsive emotion recognition systems. These findings offer promising insights for real-world applications in affective computing, mental health monitoring, and adaptive human-computer interaction, where precise emotion modeling plays a critical role.

Keywords: *Electroencephalography, Emotion, Feature Extraction, Hilbert Transform, Multi-Classification, Signal Processing*

1. INTRODUCTION

Emotion refers to the internal affective state, mood, or subjective experience of an individual [1]. These emotional states emerge as responses to external stimuli such as events, social interactions, or personal thoughts, and are typically accompanied by physiological, cognitive, and behavioral reactions. A wide variety of emotions—ranging from happiness, sadness, fear, anger, and surprise to love, hatred, curiosity, and disappointment—constitute essential components of human nature. These emotional responses play a significant role in daily life, influencing interpersonal relationships, decision-making processes, learning, memory, and overall behavior. In recent years, there has been a growing interest in recognizing and analyzing these emotional states, particularly for applications in human-machine interfaces, which aim to create seamless interaction channels between humans and intelligent systems [2]. Conventional emotion recognition methods often rely on external cues such as voice intonation, facial expressions, or posture. However, such approaches are vulnerable to intentional suppression or masking of emotions, potentially leading to inaccurate interpretations. To overcome this limitation, researchers have turned to physiological signals, including electrooculogram, respiration patterns, galvanic skin response, and especially electroencephalography (EEG), which captures the brain's electrical activity in real time [3]. EEG signals, which reflect neural communication via fluctuations in voltage across the scalp, are particularly promising for emotion recognition, as they originate directly from the central nervous system—the primary control center of the body [4]. These signals provide a high temporal resolution,

***Corresponding Author:** Hatice OKUMUS, haticeokumus@ktu.edu.tr

enabling fine-grained analysis of dynamic emotional processes.

The growing interest in EEG-based emotion recognition has led to the development and use of various publicly available EEG datasets. One of the most widely used is the SEED dataset [5,6], which has served as the foundation for numerous studies. Li et al., for instance, proposed a hierarchical convolutional neural network (HCNN) using differential entropy features arranged in 2D maps to maintain spatial electrode topology, achieving a classification accuracy of 86.20% [7]. Asghar et al. adopted a deep neural network based on the AlexNet architecture and spectrogram preprocessing, obtaining 93.80% accuracy with an SVM classifier [8]. Similarly, Cheah et al. applied ResNet18 to raw EEG signals, yielding a 93.42% accuracy in classifying emotions into three categories [9]. Building on these approaches, Xiao et al. developed a four-dimensional attention-based neural network (4D-aNN) that dynamically weighted brain regions and frequency bands, achieving 95.39% accuracy [10]. In another study, Jin et al. examined both power spectral density (PSD) and differential entropy (DE) features, reporting accuracies of 85.24% and 94.72%, respectively, using the SEED dataset [11].

In addition to SEED, the DREAMER [12] and DEAP [13] datasets have been widely adopted. Song et al. reported average recognition accuracies of 90.4% in subject-dependent and 79.95% in subject-independent settings on SEED, while achieving 86.23%, 84.54%, and 85.02% for valence, arousal, and dominance respectively on DREAMER [14]. Zhang et al. proposed a Graph Convolutional Backbone (GCB) network with a Broad Learning System (BLS), which achieved 94.24% accuracy using DE features on SEED [15]. Li et al. introduced a spatiotemporal demographic network model employing adaptive time windows and GRU layers, achieving 68.28% and 71.48% accuracy for valence and arousal on the DEAP dataset [16]. Lin et al. developed a Dual-Scale EEG Mixer (DSE-Mixer) combining brain region and electrode mixing mechanisms, achieving over 95% accuracy in binary classifications, and between 89.77% and 93.35% in four-class tasks [17]. Furthermore, Gao et al. employed a CNN architecture optimized using a novel GPSO algorithm for hyperparameter tuning, achieving an average accuracy of 92.00% [18].

Despite the notable progress in the field, most existing studies have focused on binary or quadrant-based emotional categorizations, limiting their sensitivity to intermediate affective states. To address this, the current study proposes a ternary-level classification approach for both valence and arousal dimensions, offering a more granular understanding of emotion dynamics. EEG data from ten randomly selected participants in the DEAP dataset were analyzed. The recordings were segmented into time windows, and features were extracted using the Hilbert Transform (HT), which captures instantaneous signal characteristics such as amplitude and phase. These features were then input into a feed-forward neural network (FNN) for classification. To provide a comprehensive performance comparison, additional classifiers—k-nearest neighbors (k-NN) and random forest (RF)—were also employed. All experimental procedures were conducted using MATLAB 2023.

The proposed framework achieved impressive results, with mean classification accuracies of 99.13% for arousal and 99.50% for valence, significantly outperforming many existing approaches. These findings underscore the potential of ternary-level EEG-based emotion recognition systems to enhance affective computing and enable more adaptive, responsive human-machine interactions.

The rest of this paper is organized as follows: Section 2 outlines the experimental design, methodology, and data preprocessing steps. Section 3 presents the experimental results. Section 4 provides a detailed comparison with existing classification methods and discusses the implications of the findings. Finally, Section 5 offers concluding remarks and directions for future research.

2. MATERIAL AND METHODS

2.1. Data Description

Sander Koelstra et al. [13] developed a multimodal dataset called DEAP, which includes EEG and physiological signals. This dataset, derived from recordings of 32 participants aged between 19 and 37 years, maintained a balanced male-female ratio. In this study, a subset of ten participants was randomly selected from the original pool of 32 individuals included in the DEAP dataset. The primary objective of

this selection was to conduct a controlled yet representative investigation into multi-level emotion classification. By narrowing the focus to ten subjects, a balanced trade-off was achieved between computational feasibility and data variability. Furthermore, the emotion ratings provided by each participant were used to label their responses into three discrete classes—low, medium, and high—based on their individual valence and arousal scores. This ternary classification strategy was chosen to reflect the complexity of human emotional states beyond binary schemes and to enable more nuanced modeling of affective patterns in EEG signals.

Each participant was exposed to 40 videos with emotional content, selected manually from a pool of 120 music videos with affective tags obtained from last.fm. The videos were selected using a web-based subjective emotion rating interface. All videos were 1 minute in length and contained music content. EEG data were recorded at a sampling rate of 512 Hz using 32 active AgCl electrodes according to the international 10-20 system shown in Figure 1. In addition, 13 peripheral physiological signals were recorded, including GSR, respiratory amplitude, skin temperature, electrocardiogram, blood volume by plethysmograph, electromyograms of the zygomatic and trapezius muscles, and electrooculography (EOG). The synchronization of EEG with emotion data began with the display of a fixation cross on the screen, with the participant being instructed to relax for 2 minutes. Each participant was then presented with 40 one-minute videos on a trial-by-trial basis, preceded by a 2-second progress screen and a 5-second fixation cross for relaxation. Due to the highly subjective nature of emotional transition states, participant ratings were used to mark induced emotions.

The processed EEG recordings in the DEAP dataset were down-sampled to 128 Hz, and eye blink artefacts were removed using blind source separation. A band-pass frequency filter from 4.0 to 45.0 Hz was applied, and the data were averaged to the common reference before being segmented into 60-second trials with a 3-second pre-trial baseline (from the 5-second baseline recording). Participants' ratings were provided separately for valence, arousal, and dominance. DEAP and SEED are the two most widely used publicly available EEG emotion datasets, both of which use audiovisual stimuli to elicit emotion. While the DEAP dataset has a larger number of EEG recordings and physiological signals, the SEED dataset has a higher spatial resolution of EEG recordings due to a larger number of electrodes. The SEED dataset used 15 different video clips with a maximum duration of 4 minutes, in contrast to the DEAP dataset which used 40 different 1-minute video clips. Furthermore, the SEED dataset used a categorical emotion model, while the DEAP dataset used a dimensional emotion model. The proposed method was only tested on the DEAP datasets.

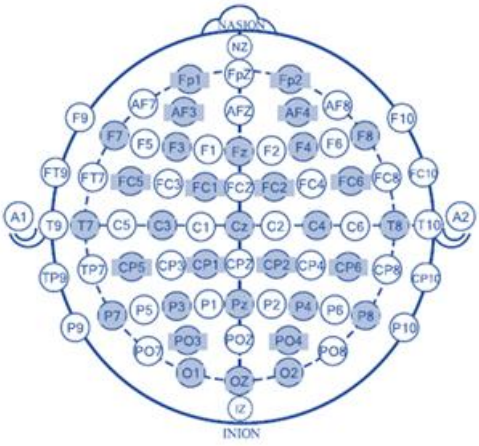

Figure 1. EEG electrode positions [19]

2.2. Methods

The proposed methodology comprises four distinct stages, each of which is integral to the comprehensive analysis of emotional responses. The general flowchart illustrating the relationship

between these stages is shown in Figure 2. First, a critical aspect is the establishment of three-level labels for each emotion, strategically segmenting the emotional spectrum into low, moderate and high intensity. This segmentation is crucial for the subsequent stages of the analysis process [20]. Following the careful categorization of emotions, the second step is to segment the data by applying a time window. This temporal segmentation of EEG signals is essential to capture nuanced fluctuations in emotional states over specific intervals. Temporal segmentation facilitates a granular examination of emotional dynamics, allowing for more detailed analysis. An example of temporal segmentation is shown in Figure 3.

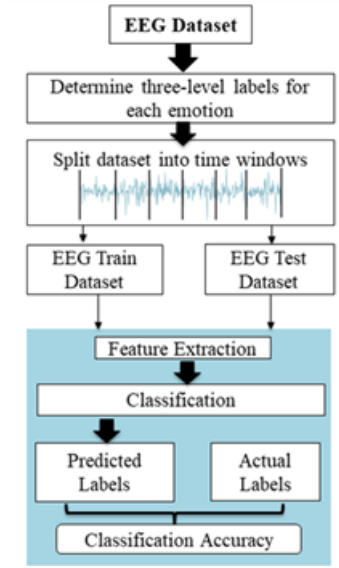

Figure 2. General flow chart of the methodology proposal

In this study, each 60-second EEG segment was divided into six non-overlapping windows of 10 seconds. The rationale behind selecting a 10-second window was to maintain a meaningful balance between signal stability and temporal resolution. Very short windows tend to reflect transient artifacts or momentary fluctuations that may not correspond to stable emotional states. Conversely, significantly longer windows may smooth out essential temporal variations, potentially diminishing the discriminative power of the extracted features. Therefore, a 10-second window was deemed optimal for preserving the integrity of emotional patterns while providing a sufficient number of samples for robust feature extraction and classification. This decision also ensured consistency across all participants and trials, which is essential for reliable performance evaluation.

Figure 3. Temporal segmentation of EEG signals

The third stage of the proposed method involves extracting relevant features from the segmented data. This step is crucial for identifying distinctive patterns and characteristics within the EEG signals that are indicative of different emotional intensities. Feature extraction acts as a bridge between the raw data and the subsequent classification process, ensuring that relevant information is used effectively. The final step is to classify the pre-processed data into discrete emotional classes. Specifically, EEG signals related to arousal and valence emotions are stratified into three distinct levels corresponding to low, moderate and high emotional intensity. The assignment of labels is derived from participants' ratings, in which each emotion is systematically evaluated. A meticulous approach is taken, whereby if individuals give a rating

within the range of 0-3, the label is designated as low; if the rating falls between 3-6, the label is classified as moderate; and if the rating extends from 6-9, the label is designated as high. It is important to emphasize that this categorization methodology is closely linked to the subjective ratings provided by the participants, reflecting the diverse range of emotional experiences and responses within the population studied. Through this multifaceted approach, the proposed method seeks to provide a nuanced and comprehensive understanding of emotional dynamics as manifested in EEG signals.

The EEG data under consideration were acquired from 32 channels, recorded at a sampling rate of 128 Hz, and each data segment had a duration of 60 seconds, resulting in a total of 1 trial. Expressing the data format as trial × number of channels × samples, the data size for the 60 second interval is 1×32×7680. For temporal analysis, the EEG data were then divided into 10 second windows. This temporal segmentation resulted in a total of 6 trials, with each trial having a data size of 6×32×1280. In the analysis pipeline, features essential for the subsequent classification process were extracted from the EEG signals using the HT method. The extracted features were then subjected to classification using three different algorithms, FNN, k-NN and RF. The use of multiple classification algorithms contributes to the robustness and reliability of the test results. In order to assess the performance of the classification models, all results were calculated by averaging the results after a 10-fold cross-validation. This approach ensures a comprehensive evaluation, taking into account variations in the dataset through multiple rounds of cross-validation. It is worth noting that the computational infrastructure used for these processes was a computer with a configuration of 16 GB RAM and a 2.92 GHz Intel Core i7 processor. This hardware configuration is essential to meet the computational demands of the feature extraction, classification and cross-validation processes, thus contributing to the accuracy and efficiency of the analyses performed in this study.

Furthermore, the continuous self-assessment scores for valence and arousal were discretized into three ordinal levels—low, medium, and high—using participant-specific thresholds. After this labeling process, the distribution of samples across the ternary classes was examined. While the resulting class frequencies were not perfectly balanced, no extreme skew was observed. To address potential bias caused by moderate class imbalance, a 10-fold cross-validation strategy was adopted, ensuring that each fold retained a representative distribution of class labels. This procedure enhances the model's robustness by exposing it to diverse subsets of the data and mitigating the risk of overfitting to overrepresented classes.

2.2.1. Feature Extraction Using Hilbert Transform

Data mining and machine learning rely heavily on feature extraction, a technique that is integral to discovering and extracting attributes from data sets to improve their relevance and usability [21]. Essentially, the aim is to transform complex or high-dimensional data into low-dimensional, meaningful and unambiguous features. In the context of this study, feature extraction was performed using HT. In the field of EEG signal processing, the extraction of significant features is of paramount importance in revealing underlying patterns and information essential for subsequent analysis [22]. The HT proves to be a crucial tool in this regard. Particularly being adept at analyzing time-varying signals, the HT facilitates the extraction of amplitude and phase information from complex signals such as EEG data. By applying the HT to EEG recordings, researchers can capture dynamic changes in brain activity and identify temporal patterns associated with specific cognitive or emotional states. Incorporating the HT into feature extraction improves our understanding of the temporal dynamics inherent in EEG signals. This in turn facilitates the development of robust models for various tasks, including but not limited to emotion recognition, cognitive state classification, and diagnosis of neurological disorders.

The HT, introduced by David Hilbert in the early 20th century, has proven to be a versatile mathematical operation with applications spanning diverse fields such as telecommunications, physics, and biomedical signal processing [23]. Its efficacy is particularly notable in the analysis of time-varying signals, where the representation of frequency as a rate of change in phase over time facilitates the investigation of non-stationary signals [22]. In the context of raw data, which inherently encompasses a multitude of frequencies evolving over time, the HT simplifies the representation of these frequencies in

the frequency domain. Notably, it introduces a $\pm 90^{\circ}$phase shift based on the sign of each frequency component within a function. In the case of this study, the EEG signal, denoted as $k(l)$, undergoes HT processing. This involves convolving the signal with $h(t) = 1/\pi l$, as outlined in Equation 1. The impulse response of $h(l)$ is detailed in Equation 2.

$$H\{k(t)\} = \hat{k}(l) = \mathrm{k}(l) * \frac{1}{\pi l} = \frac{1}{\pi}\int_{-\infty}^{\infty} \frac{\mathrm{k}(\tau)}{l-\tau} d\tau \tag{1}$$

$$H(\omega) = F[h(l)] = -i * sign(\omega) \tag{2}$$

In Equation 2, the impulse response of the signal exhibits a phase shift of $+i$ for $\omega < 0$ and $-i$ for $\omega > 0$. This indicates that the HT introduces a $+90$ degree shift for negative frequency components of the signal $k(l)$ and a -90 degree shift for positive frequency components. Adhering to the principle of causality, the HT of a signal $k(l)$ is associated with both its real and imaginary parts, as elucidated in Equation 3. The averaging of the real parts of $\hat{k}(l)$, denoted as (HT_{feat}), is mathematically expressed in Equation 4. Here, n represents the length of $\hat{k}(l)$. In the present study, the values of (HT_{feat}) are employed as features, effectively representing EEG trials. This utilization of (HT_{feat}) as features in the context of EEG trials serves to encapsulate the temporal dynamics revealed through the HT.

$$\widehat{kn}(l) = r(\widehat{kn}(l)) + i(\widehat{kn}(l)) \tag{3}$$

$$HT_{feat} = \frac{\sum_{i=1}^{n} r(\widehat{kn}_i(l))}{n} \tag{4}$$

In this study, the HT was utilized to extract features from EEG signals, owing to its effectiveness in capturing both the instantaneous amplitude and phase components of neural activity. These characteristics are essential for decoding the temporal dynamics of emotional states, which often manifest in subtle changes in neural oscillations. Unlike Fourier Transform, which is constrained by the assumption of signal stationarity and lacks temporal resolution, HT provides an analytic signal representation that maintains the non-stationary and nonlinear properties of EEG. Compared to Wavelet Transform, HT also offers a simpler implementation framework without the requirement for predefined basis functions, and with more direct access to phase-related features that are known to be informative in affective computing contexts.

2.2.2. Classification Procedure

Both data mining and machine learning require classification techniques [24]. Classification is essentially the process of assigning components in a data collection to a particular class or category. This process assigns components to specific classes based on characteristics in the existing data collection. Classification algorithms discover patterns throughout the learning process and accurately categories subsequent cases. The error matrix (or confusion matrix) is a table used to evaluate the performance of a classification model. This matrix shows the relationship between the actual and expected classes of the model. A three-class error matrix is often divided into four categories: true positive (yP), true negative (yN), false positive (hP) and false negative (hN). yP, a true positive occurs when the model correctly predicts a sample to be positive, yN, a true negative occurs when the model correctly predicts a sample to be negative, hP, a false positive occurs when the model incorrectly classifies a sample as positive, and hN, a false negative occurs when a model incorrectly predicts a sample to be negative [25]. The three-class confusion matrix is shown in Table 1. These metrics allow us to evaluate the performance of a classification model from different perspectives. CA is the overall accuracy rate, sensitivity (SeN) is how well one class is recognized, and specificity (SeP) is how well other classes are recognized. CA, SeN and SeP are also given in equations 5, 6 and 7, respectively.

To evaluate the robustness of the proposed model, 10-fold cross-validation was employed. This technique ensures that each segment of the data is used in both training and validation phases, minimizing bias and improving the model's generalizability. This method provides a balanced compromise between training size and evaluation reliability.

Table 1. Class labels

Confusion Matrix		Predicted Classes		
		$Class_1$	$Class_2$	$Class_3$
Actual Classes	$Class_1$	yP	hP_1	hP_2
	$Class_2$	hN_1	yP	hP_3
	$Class_3$	hN_2	hN_3	yP

$$CA = \frac{yP}{\mathrm{yP}+hP_1+hP_2+hP_3+hN_1+hN_2+hN_3} x100 \quad (5)$$

$$SeN = \frac{yP}{\mathrm{yP}+hN_1+hN_2+hN_3} x100 \quad (6)$$

$$SeP = \frac{yP}{\mathrm{yP}+hP_1+hP_2+hP_3} x100 \quad (7)$$

2.2.2.1. Feedforward Neural Network

FNN is a neural network model commonly used in artificial intelligence and machine learning. This paradigm features a forward flow in the information processing process, meaning that information starts in an input layer and progresses through subsequent layers to the output layer [26]. FNN consists of three basic layers, each of which consists of many neurons (or nodes): the input layer, the hidden layer(s), and the output layer. The input layer contains the data that the model receives from the outside world. Hidden layers are used to extract features from this input and improve the model's learning capabilities. The output layer is responsible for the final prediction or classification results of the model. Each neuron generates an output by multiplying its inputs with weights and sending them through an activation function. This is done using backward learning algorithms, which change the parameters of the model as it learns. FNNs have a wide range of applications. They have been used effectively in a wide range of applications, including classification, regression, pattern recognition and prediction [27]. When discussing FNNs in academic articles, aspects such as activation functions, number of layers, number of neurons, learning methods and performance evaluation measures are often highlighted. In addition, analyses of the model's effectiveness and learning capabilities in a given application provide valuable academic information.

In this study, the FNN model was developed using MATLAB's feedforwardnet function, which is part of the Deep Learning Toolbox (formerly known as Neural Network Toolbox). The model was configured with default parameters, except that the maximum number of training epochs was set to 100. All experiments were conducted with 10-fold cross-validation, and the reported metrics represent the averaged results over the folds.

2.2.2.2. k-Nearest Neighbors

The k-NN algorithm is a supervised machine learning approach utilized for classification tasks. Its operation involves assigning a label to a test trial based on the classification of its nearest neighbor(s) within the training set. The algorithm strives to assess the distance or similarity between instances in the training and test datasets. This study employed various distance measures, including Euclidean, Cosine, City Block, and Correlation [28], to determine the proximity between trials. Notably, the Euclidean distance yielded the most favorable outcomes among these measures. The Euclidean distance (EUC)

between two trials is quantified using Equation 8, where b and v represent n points, and EUC denotes the Euclidean distance. The selection of an appropriate distance measure is crucial in influencing the algorithm's performance, and in this case, the study found the Euclidean distance to be the most effective [29]. Another key consideration in the k-NN method is determining the value of the k parameter. This parameter indicates the number of the nearest neighbors to be considered in the classification process. In the present study, the optimal value of k was systematically determined for each modality and subject in each run, using the cross-validation method. This meticulous approach ensured the robustness of the k-NN model, and subsequent test classifications were performed accordingly. The systematic calculation of optimal k-values contributes to the adaptability and effectiveness of the model across different datasets and scenarios.

$$EUC(b,v) = \sqrt{\sum_{i=1}^{n}(y_{bi} - y_{vi})^2} \tag{8}$$

2.2.2.3. Random Forest Algorithm

The RF is a powerful and popular ensemble learning approach in machine learning [30]. An ensemble learning technique combines many separate models to make predictions, and RF is known for its adaptability and resilience. The algorithm is a member of the decision tree family of techniques and is characterized by its ability to generate a large number of decision trees during training. The RF generates a forest of decision trees, each of which is created using a portion of the training data and features. Randomization in the selection of both data instances and features increases the diversity among the constituent trees, which helps the model resist overfitting and improves generalization performance on previously unknown data. In a RF, predictions are made by aggregating the outputs of individual trees. For classification tasks, the method uses a majority voting mechanism, but for regression tasks it takes the average of the predictions. This ensemble-based technique allows RF to capture complicated correlations within the data, providing a robust solution to a wide range of machine learning problems. One of the main advantages of the RF is its ability to handle large, high-dimensional datasets containing both categorical and numerical variables. In addition, its inherent resistance to overfitting, ease of implementation, and adaptability to different domains contribute to its prominence in academic research and practical applications [31]. The versatility and effectiveness of the algorithm make it a useful tool for solving complicated problems in a wide range of disciplines, including finance, healthcare and image identification.

3. DEPICTION OF EXPERIMENTAL RESULTS

In this study, an illustrative graph is used to convey the research results, as exemplified by the subject-specific bar graphs shown in Figure 4. Each graph shows the 10-fold cross-validation results for three classification algorithms: k-NN, RF and FNN, applied to 10 different subjects. The individual columns within the bar graph correspond to the CA, SeP and SeN achieved for each subject, labelled $S_1, S_2, S_3, S_4, S_5, S_6, S_7, S_8, S_9$ and S_{10}, representing subject 1 to subject 10 respectively. The demarcation lines between the bar columns act as boundary indicators, with values of 20, 40, 60, 80 and 100 delineating the CA, SeP and SeN scale. In the figure, Subject 10 achieves a value of 88.68% according to the SeP metric, whereas a separate calculation reveals a value of 75.82% for Subject 6 based on the SeN metric. Notably, given that the experiment involved 10 different subjects, the totality of the experimental results, including the subject-specific test CA, SeP and SeN results for each classifier, is systematically presented using these graphical representations to enhance the visual clarity and comprehension of the study results.

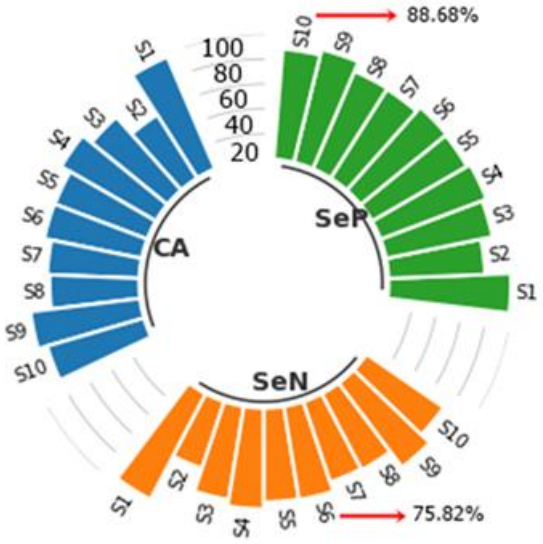

Figure 4. General presentation of topic-specific bar graphs

4. RESULTS

The primary aim of the current investigation was to overcome this limitation by assessing the classification accuracy and efficacy of different EEG feature sets in discriminating emotional states, with a particular focus on valence and arousal. Initially, a crucial aspect was the curation of a 3-class EEG dataset, where the establishment of three-level labels for each emotion played a pivotal role in strategically segmenting the emotional spectrum into low, moderate and high intensities. The dataset was then segmented into 6-second intervals. Features based on the HT were then extracted from the segmented signals, and the resulting features underwent classification using FNN, with subsequent labelling of unknown test trials. The proposed methodology for the ternary-level emotion dataset, comprising 10 randomly selected subjects, was applied independently to each subject, targeting valence and arousal emotions within 6 second time segments. The entirety of the EEG channels was used in all classification processes, and the resulting classification results were computed for metrics such as CA, SeN, and SeP. The subject-specific bar chart in Figure 5 shows the classification results for each metric using FNN.

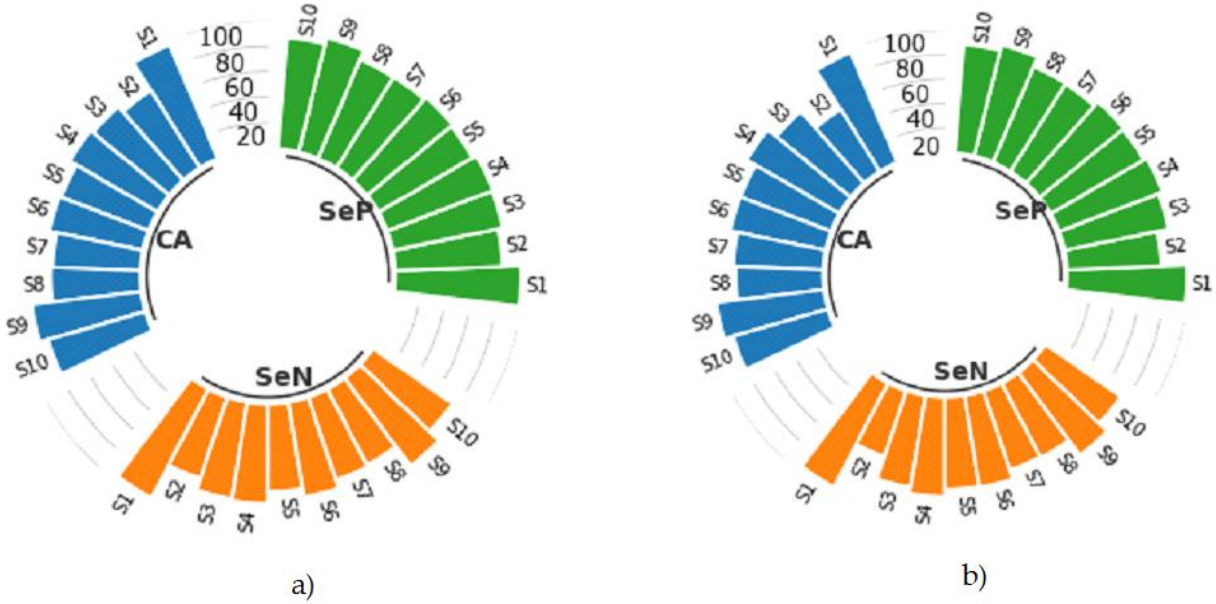

Figure 5. Classification results for a) valence and b) arousal emotion with FNN

As shown in the figure, the optimal test CA values for valence were found to be 100.00% for subjects S1, S3 and S10 respectively. In contrast, the lowest test CA of 98.75% was observed for subject S6 and S7. Furthermore, the highest test CAs for arousal were calculated as 100.00% for subjects S5 and S6 while the least favorable test CAs were documented as 97.50% for subjects S10. In order to provide a comprehensive comparison of the classification results, we also used k-NN and RF algorithms to compute classification results for valence and arousal emotions. The results for k-NN are shown in Figure 6, while those for RF are shown in Figure 7. As can be seen in Figure 6, the best CA was computed at 97.08% for S1, while the worst CA was determined at 69.16% for S7 for valence. Conversely, in Figure 6, the highest CA was calculated at 97.50% for S1, while the lowest CA was recorded at 60.00% for S2 for arousal. In Figure 7, the CA was calculated at 95.83% for S1, while the least favorable CAs were determined at 77.91% for both S2 and S7 in the context of valence classification. Conversely, within the same figure, the highest CAs were calculated at 94.58% for S1 and S4, while the lowest CA was recorded at 74.16% for S2 in the context of arousal classification. In addition, to highlight the effectiveness of using the FNN classifier to classify valence and arousal emotions, we present the mean classification results in Table 2. For valence emotion, the average values for k-NN were calculated as 77.91%, 76.08% and 87.97% for CA, SeN and SeP, respectively. In contrast, the corresponding averages for RF were 85.75%, 82.87% and 91.89%. Similarly, for arousal emotion, the means for k-NN were 79.66%, 75.68% and 88.18%, while for RF they were 85.79%, 81.53% and 91.27%. In particular, when examining the results in the table, it becomes clear that the most favorable average classification results are obtained with FNN. Specifically, for valence the averages were 99.50%, 99.52% and 99.73% for CA, SeN and SeP, respectively, whereas the averages were 99.13%, 98.96% and 99.47% for arousal emotion. These results highlight the effectiveness of the FNN in discriminating signals within the proposed experimental paradigm of this study.

Table 2. Result of classifying mean CA, SeN and SeP metrics for valence and arousal

Classifier	Valence			Arousal		
	CA	SeN	SeP	CA	SeN	SeP
***k*-NN**	77.91	76.08	87.97	79.66	75.68	88.18
RF	85.75	82.87	91.89	85.79	81.53	91.27
FNN	**99.50**	99.52	99.73	**99.13**	98.96	99.47

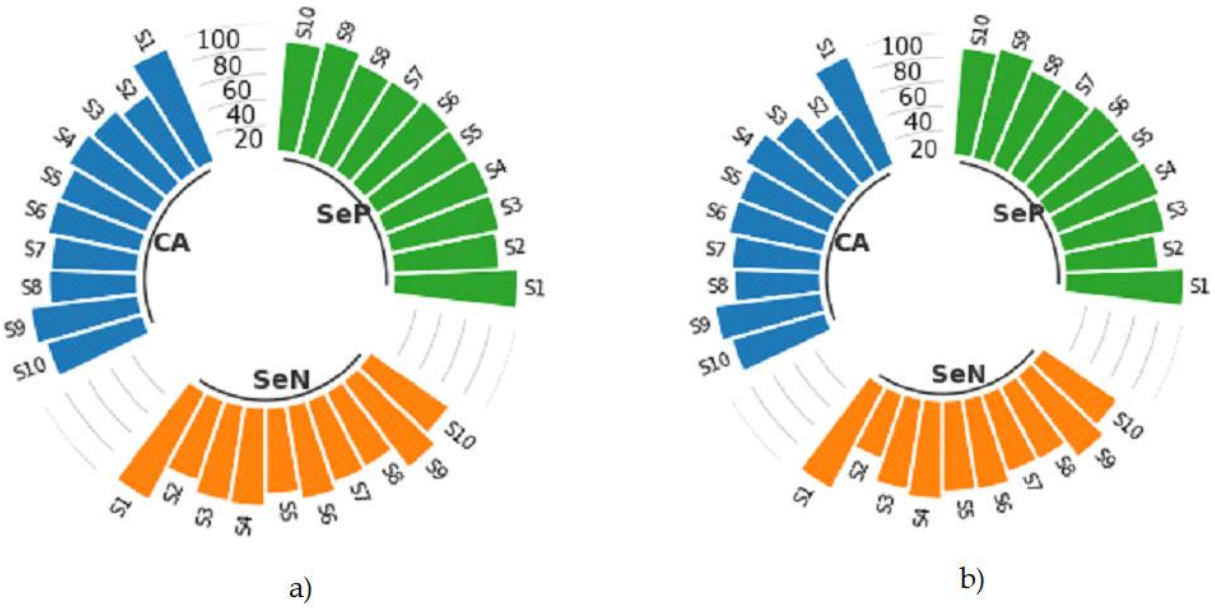

Figure 6. Classification results for a) valence and b) arousal emotion with k-NN

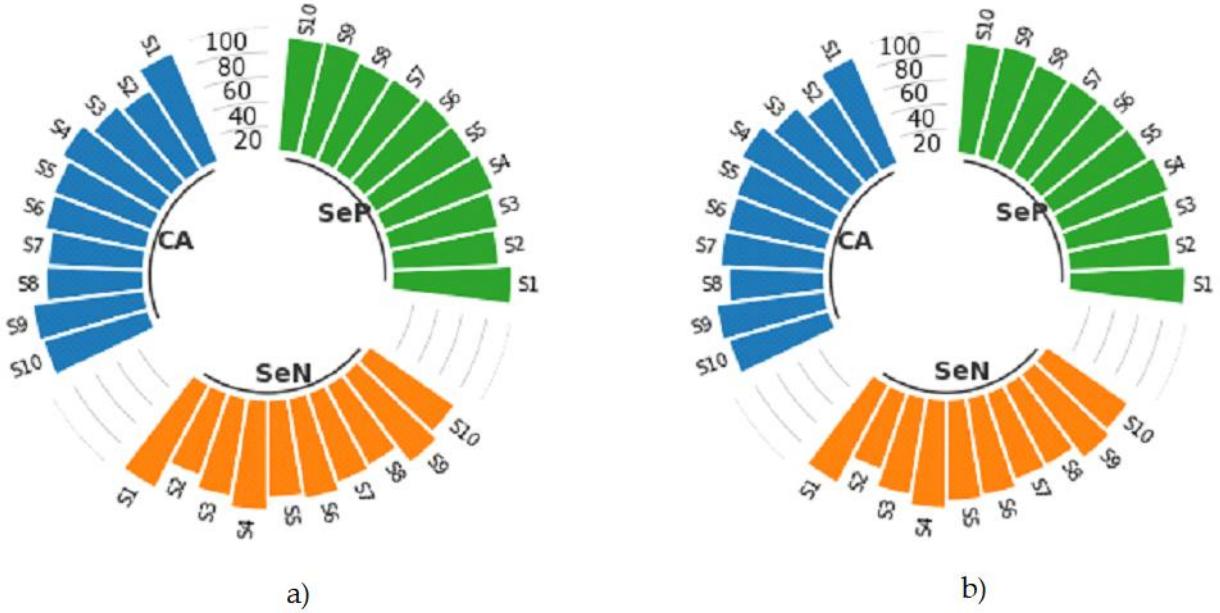

Figure 7. Classification results for a) valence and b) arousal emotion with RF

As shown in Table 3, the subject-wise and average confusion matrix results for valence classification with FNN indicate that the model performed particularly well in distinguishing high valence levels. For instance, the number of correctly classified high-valence instances was consistently high across most subjects. This trend suggests that the features extracted for high valence states were more distinguishable, possibly due to higher signal-to-noise ratio or stronger EEG activation patterns associated with high arousal-affective states.

In contrast, low valence samples showed more variability across subjects. For example, S10 had only 1.80 correctly classified low-valence samples, while S6 achieved 8.80. Some misclassifications were observed between low and adjacent medium valence classes, particularly in S9 and S6, where 0.1 and 0.2 samples were misclassified, respectively. This may be attributed to overlapping feature representations between low and medium emotional states, which are often less separable in EEG-based studies.

Medium valence classes generally showed high accuracy, with almost no confusion across categories. However, Subjects 2 and 7 had 0.1 misclassifications from medium to low, indicating a subject-dependent variability in class separability.

Similarly, in Table 4, arousal classification with FNN yielded highly accurate results for high arousal across multiple subjects. For instance, S1 (14.3), S3 (7.1), S5 (10.8), S6 (12.0), and S10 (12.5) showed nearly perfect or perfect classification in the high arousal category. Misclassifications primarily occurred in medium arousal samples, such as in S1 and S2, where 0.1–0.2 samples were misclassified into the high class. This is expected due to the gradual transition in physiological patterns between medium and high arousal states. Interestingly, the medium arousal class showed the highest variation in classification accuracy. For example, S4 had the highest correct classification count for medium arousal (15.9), while S9 and S10 had lower accuracy due to confusion with low and high classes. The low arousal class was generally well classified across subjects, with particularly strong performance in S8 (7.8), S9 (6.4), and S3 (4.2), but some instances in S10 and S6 were misclassified into the medium or high classes. In both valence and arousal confusion matrices, a clear trend is observed where extreme classes (low and high) tend to be classified more accurately than the intermediate (medium) class. This can be attributed to the relatively blurred emotional boundaries.

Table 3. Subject-wise and average confusion matrix results for valence classification with FNN

S1		Predicted Classes		
		low	medium	high
Actual Classes	low	7.20	0.00	0.00
	medium	0.00	6.00	0.00
	high	0.00	0.00	10.80

S2		Predicted Classes		
		low	medium	high
Actual Classes	low	3.60	0.00	0.00
	medium	0.10	8.30	0.00
	high	0.00	0.00	12.00

S3		Predicted Classes		
		low	medium	high
Actual Classes	low	5.40	0.00	0.00
	medium	0.00	11.40	0.00
	high	0.00	0.00	7.20

S4		Predicted Classes		
		low	medium	high
Actual Classes	low	3.00	0.00	0.00
	medium	0.00	10.8	0.00
	high	0.00	0.10	10.10

S5		Predicted Classes		
		low	medium	high
Actual Classes	low	3.00	0.00	0.00
	medium	0.00	11.30	0.10
	high	0.00	0.00	9.60

S6		Predicted Classes		
		low	medium	high
Actual Classes	low	8.80	0.00	0.20
	medium	0.00	6.00	0.00
	high	0.10	0.00	8.90

S7		Predicted Classes		
		low	medium	high
Actual Classes	low	6.50	0.10	0.00
	medium	0.10	8.30	0.00
	high	0.10	0.00	8.90

S8		Predicted Classes		
		low	medium	high
Actual Classes	low	6.60	0.00	0.00
	medium	0.00	4.80	0.00
	high	0.00	0.10	12.50

S9		Predicted Classes		
		low	medium	high
Actual Classes	low	4.70	0.00	0.10
	medium	0.00	7.10	0.10
	high	0.00	0.00	12.00

S10		Predicted Classes		
		low	medium	high
Actual Classes	low	1.80	0.00	0.00
	medium	0.00	12.00	0.00
	high	0.00	0.00	10.20

We also conducted a comparison with studies in the literature that used the same dataset. The methods and results of these studies are presented in Table 5. Looking at the results in the table, it is clear that previous research efforts have opted to create a common dataset with four classes combining valence and arousal, rather than clearly classifying valence and arousal emotions. In contrast, the current study classified valence and arousal emotions into three distinct levels. A review of the literature shows that the best result, with a score of 96.90%, was achieved by classifying deep learning architectures with features based on continuous wavelet transform (CWT). Conversely, in [38], the least favorable result was calculated at 69.67%, using Graph Regularized Extreme Learning. Comparing the results obtained, it is clear that the ternary classification proposed in this study makes a significant contribution to the literature, achieving test accuracies of 99.50% and 99.13%.

Furthermore, Although the class structures differ among studies, we report the comparison to demonstrate the robustness of our model under a more fine-grained ternary classification setting, which is inherently more complex than binary class divisions.

4. CONCLUSIONS

This study implemented and evaluated a methodological framework to fulfil its primary objective to assess the classification accuracy and efficacy of different EEG feature sets in discriminating emotional

states, with a particular focus on valence and arousal. The research began with the curation of a 3-class EEG dataset, strategically incorporating three-level labels indicative of emotional intensity. This was followed by temporal segmentation into 10-second intervals, which facilitated the extraction of HT-based features for subsequent classification using FNN. Application of the ternary-level emotion dataset to 10 subjects produced subject-specific bar charts depicting FNN classification results. In addition, a comparative analysis with related studies using the same dataset revealed a departure from the conventional approach of creating a common dataset with four classes combining valence and arousal emotions. Instead, our study adopted a more refined structure by distinctly categorizing valence and arousal emotions into three levels each. This enhanced labeling scheme improved the granularity and interpretability of emotion classification results.

Table 4. Subject-wise and average confusion matrix results for arousal classification with FNN

S1		Predicted Classes		
		low	medium	high
Actual Classes	low	4.20	0.00	0.00
	medium	0.00	5.30	0.10
	high	0.10	0.00	14.30

S2		Predicted Classes		
		low	medium	high
Actual Classes	low	3.00	0.00	0.00
	medium	0.00	11.80	0.20
	high	0.00	0.00	9.00

S3		Predicted Classes		
		low	medium	high
Actual Classes	low	4.20	0.00	0.00
	medium	0.00	12.60	0.00
	high	0.00	0.10	7.10

S4		Predicted Classes		
		low	medium	high
Actual Classes	low	2.40	0.00	v
	medium	0.00	15.90	0.30
	high	0.00	0.10	5.30

S5		Predicted Classes		
		low	medium	high
Actual Classes	low	3.00	0.00	0.00
	medium	0.00	10.20	0.00
	high	0.00	0.00	10.80

S6		Predicted Classes		
		low	medium	high
Actual Classes	low	3.60	0.00	0.00
	medium	0.00	8.40	0.00
	high	0.00	0.00	12.00

S7		Predicted Classes		
		low	medium	high
Actual Classes	low	3.60	0.00	0.00
	medium	0.00	5.400	0.00
	high	0.00	0.2	14.80

S8		Predicted Classes		
		low	medium	high
Actual Classes	low	7.80	0.00	0.00
	medium	0.10	5.30	0.00
	high	0.00	0.00	10.80

S9		Predicted Classes		
		low	medium	high
Actual Classes	low	6.40	0.00	0.20
	medium	0.00	4.20	0.00
	high	0.10	0.00	13.10

S10		Predicted Classes		
		low	medium	high
Actual Classes	low	1.60	0.10	0.10
	medium	0.00	9.30	0.30
	high	0.00	0.10	12.50

Table 5. Comparison of classification accuracy with prior studies

References	Procedure			
	Features Method	**Classifier Method**	**Classes**	**CA (%)**
[19]	Time domain features	CNN	4	76.77
[32]	Empirical mode decomposition	LSTM	4	88.42
[33]	CWT	AlexNet, ResNet-18, Vgg-19, Inception-v1, Inception-v3	4	96.90
[34]	Frequency temporal spatial	CNN-FcaNet	4	88.46
[35]	Information Potential	RF	4	71.43
[36]	Pearson correlation coefficient	CNN	4	73.10
[37]	Power spectral density, differential entropy, differential asymmetry, rational asymmetry, asymmetry and differential causality	Graph regularized Extreme Learning	4	69.67
[38]	Phase space dynamics and poincare sections	Multi-class SVM	4	81.67
[39]	Spectrograms	CNN	4	75.00
Proposed Method	HT	FNN	3	Valence:99.50 Arousal: 99.13

The model achieved exceptionally high classification accuracies—99.50% for valence and 99.13% for arousal—driven by the synergy of carefully designed methodological components. Specifically, the segmentation strategy increased training data while maintaining temporal integrity; the use of Hilbert Transform-based features enabled the extraction of rich instantaneous signal characteristics; and the neural network architecture captured relevant discriminative patterns. Together, these elements contributed to the robust performance of the proposed approach.

The presented methodology offers a solid foundation for future research into emotional state detection using advanced signal processing and classification techniques. The proposed three-level emotion classification framework has promising implications across various real-life domains. In healthcare, such models can be integrated into neurofeedback systems for emotion regulation therapies, particularly in managing anxiety, depression, or post-traumatic stress disorder (PTSD). In education, emotion-aware intelligent tutoring systems can adapt instructional content based on a learner's emotional state, enhancing engagement and learning outcomes. In the field of human-computer interaction, particularly in affective computing and virtual reality environments, real-time emotion detection can improve system responsiveness and user experience. Furthermore, the model's capacity to distinguish between low, moderate, and high emotional intensities allows for a more nuanced understanding of affective states, which is critical in continuous monitoring applications. These insights demonstrate that the model is not only technically robust but also applicable in diverse interdisciplinary settings where emotional intelligence is increasingly vital.

Despite the promising performance of the proposed model, several limitations must be acknowledged. EEG signals are prone to noise arising from muscular artifacts, environmental interference, and hardware limitations. The controlled laboratory setting may not fully reflect real-world emotional dynamics, potentially affecting ecological validity. Moreover, the use of a feed-forward neural network, although effective in static classification tasks, does not leverage temporal relationships that may exist within EEG time series. These aspects may introduce variability in classification performance and will be

systematically addressed in future investigations.

Declaration of Ethical Standards

The authors declare that all ethical guidelines including authorship, citation, data reporting, and publishing original research are followed.

Credit Authorship Contribution Statement

All authors contributed equally. Author1 contributed to the preparation of the methodology and description of the dataset, while Author2 analyzed the results and formulated the conclusions. In addition, Author1 and Author2 collaborated on data validation prior to manuscript preparation. They also contributed to drafting the manuscript.

Declaration of Competing Interest

The authors declare that there is no conflict of interest.

Funding / Acknowledgements

This research received no specific grant from any funding agency in the public, commercial, or not-for-profit sectors.

Data Availability

No data available.

REFERENCES

[1] M. G. Huddar, S. S. Sannakki, and V. S. Rajpurohit, "Attention-based multi-modal sentiment analysis and emotion detection in conversation using RNN," *Int. J. Interact. Multimedia Artif. Intell*, vol. 6, no. 6, June 2021, doi: 10.9781/ijimai.2020.07.004.

[2] W. Rahmouni, G. Bachir, and M. Aillerie, "A new control strategy for harmonic reduction in photovoltaic inverters inspired by the autonomous nervous system," *J. Electr. Eng.*, vol. 73, no. 5, pp. 310–317, September 2022, doi: 10.2478/jee-2022-0041.

[3] L. George and H. Hadi, "User identification and verification from a pair of simultaneous EEG channels using transform-based features," *Int. J. Interact. Multimedia Artif. Intell.*, vol. 5, no. 5,pp. 54-62, June 2019, doi: 10.9781/ijimai.2018.12.008.

[4] J. Wang and M. Wang, "Review of the emotional feature extraction and classification using EEG signals," *Cogn. Robot.*, vol. 1, pp. 29–40, April 2021, doi: 10.1016/j.cogr.2021.04.001.

[5] W. L. Zheng and B. L. Lu, "Investigating critical frequency bands and channels for EEG-based emotion recognition with deep neural networks," *IEEE Trans. Auton. Ment. Dev.*, vol. 7, no. 3, pp. 162–175, May 2015, doi: 10.1109/TAMD.2015.2431497.

[6] R. N. Duan, J. Y. Zhu, and B. L. Lu, "Differential entropy feature for EEG-based emotion classification," in Proc. 6th Int. IEEE/EMBS Conf. Neural Eng. (NER), San Diego, CA, USA, November 2013, pp. 81–84, doi: 10.1109/NER.2013.6695889.

[7] J. Li, Z. Zhang, and H. He, "Hierarchical convolutional neural networks for EEG-based emotion recognition," *Cogn. Comput.*, vol. 10, pp. 368–380, April 2018, doi: 10.1007/s12559-017-9533-x.

[8] M. A. Asghar et al., "EEG-based multi-modal emotion recognition using bag of deep features: An optimal feature selection approach," *Sensors*, vol. 19, no. 23, p. 5218, November 2019, doi: 10.3390/s19235218.

[9] K. H. Cheah, H. Nisar, V. V. Yap, C. Y. Lee, and G. R. Sinha, "Optimizing residual networks and VGG for classification of EEG signals: Identifying ideal channels for emotion recognition," *J. Healthcare Eng.*, vol. 1, pp. 1–10, March 2021, doi: 10.1155/2021/5599615.

[10] G. Xiao et al., "4D attention-based neural network for EEG emotion recognition," *Cogn. Neurodynamics*, vol. 16, pp. 1–14, January 2022, doi: 10.1007/s11571-021-09751-5.

[11] M. Jin, H. Chen, Z. Li, and J. Li, "EEG-based emotion recognition using graph convolutional network with learnable electrode relations," in Proc. 43rd Annu. Int. Conf. IEEE Eng. Med. Biol. Soc. (EMBC), Mexico, November 2021, pp. 5953–5957, doi: 10.1109/EMBC46164.2021.9630062.

[12] S. Katsigiannis and N. Ramzan, "DREAMER: A database for emotion recognition through EEG and ECG signals from wireless low-cost off-the-shelf devices," *IEEE J. Biomed. Health Inform.*, vol. 22, no. 1, pp. 98–107, March 2017, doi: 10.1109/JBHI.2017.2688239.

[13] S. Koelstra et al., "DEAP: A database for emotion analysis using physiological signals," *IEEE Trans. Affect. Comput.*, vol. 3, no. 1, pp. 18–31, December 2011, doi: 10.1109/T-AFFC.2011.15.

[14] T. Song, W. Zheng, P. Song, and Z. Cui, "EEG emotion recognition using dynamical graph convolutional neural networks," *IEEE Trans. Affect. Comput.*, vol. 11, no. 3, pp. 532–541, March 2018, doi: 10.1109/TAFFC.2018.2817622.

[15] T. Zhang, X. Wang, X. Xu, and C. P. Chen, "GCB-Net: Graph convolutional broad network and its application in emotion recognition," *IEEE Trans. Affect. Comput.*, vol. 13, no. 1, pp. 379–388, August 2019, doi: 10.1109/TAFFC.2019.2937768.

[16] R. Li et al., "SSTD: A novel spatio-temporal demographic network for EEG-based emotion recognition," *IEEE Trans. Comput. Soc. Syst.*, vol. 10, no. 1, pp. 376–387, January 2022, doi: 10.1109/TCSS.2022.3188891.

[17] K. Lin, L. Zhang, J. Cai, J. Sun, W. Cui, and G. Liu, "DSE-Mixer: A pure multilayer perceptron network for emotion recognition from EEG feature maps," *J. Neurosci. Methods*, vol. 401, January 2024, doi: 10.1016/j.jneumeth.2023.110008.

[18] Z. Gao, Y. Li, Y. Yang, X. Wang, N. Dong, and H. D. Chiang, "A GPSO-optimized convolutional neural networks for EEG-based emotion recognition," *Neurocomputing*, vol. 380, pp. 225–235, March 2020, doi: 10.1016/j.neucom.2019.10.096.

[19] H. Chao and L. Dong, "Emotion recognition using three-dimensional feature and convolutional neural network from multichannel EEG signals," *IEEE Sensors J.*, vol. 21, no. 2, pp. 2024–2034, September 2020, doi: 10.1109/JSEN.2020.3020828.

[20] K. Martín-Chinea, J. Ortega, J. F. Gómez-González, E. Pereda, J. Toledo, & L. Acosta, "Effect of time windows in LSTM networks for EEG-based BCIs. Cognitive Neurodynamics", vol. 17, no.2, 385-398, April 2023. doi: 10.1007/s11571-022-09832-z.

[21] S. Zhou, B. Chen, Y. Zhang, H. Liu, Y. Xiao, and X. Pan, "A feature extraction method based on feature fusion and its application in the text-driven failure diagnosis field," *Int. J. Interact. Multimedia Artif. Intell.*, vol. 6, no. 4, pp. 121-130, December 2020, doi: 10.9781/ijimai.2020.11.006.

[22] E. Ergün and O. Aydemir, "A Hybrid BCI Using Singular Value Decomposition Values of the Fast Walsh–Hadamard Transform Coefficients," *IEEE Trans. Cogn. Dev. Syst.*, vol. 15, no. 2, pp. 454–463, October 2020, doi: 10.1109/TCDS.2020.3028785.

[23] H. M. Emara et al., "Hilbert transform and statistical analysis for channel selection and epileptic seizure prediction," *Wireless Pers. Commun.*, vol. 116, pp. 3371–3395, January 2021, doi: 10.1007/s11277-020-07857-3.

[24] E. Ergün, "Artificial Intelligence Approaches for Accurate Assessment of Insulator Cleanliness in High-Voltage Electrical Systems," *Electr. Eng.*, pp. 1–16, August 2024, doi: 10.1007/s00202-024-02691-.

[25] E. Yavuz, and Ö. Aydemir, "Classification of EEG based BCI signals imagined hand closing and opening". In IEEE 40th International Conference on Telecommunications and Signal Processing (TSP), pp. 425-428, July 2017, doi: 10.1109/TSP.2017.8076020.

[26] D. Svozil, V. Kvasnicka, and J. Pospichal, "Introduction to multi-layer feed-forward neural networks," *Chemom. Intell. Lab. Syst.*, vol. 39, no. 1, pp. 43–62, November 1997, doi: 10.1016/S0169-7439(97)00061-0.

[27] H. Choubey and A. Pandey, "A combination of statistical parameters for the detection of epilepsy and EEG classification using ANN and KNN classifier," *Signal Image Video Process.*, vol. 15, no. 3, pp. 475–483, April 2021, doi: 10.1007/s11760-020-01767-4.

[28] E. Ergün, "Deep learning-based multiclass classification for citrus anomaly detection in Agriculture". *Signal Image Video Process*, vol. 18, pp. 8077–8088, July 2024. doi: 10.1007/s11760-024-03452-2.

[29] E. Yavuz, and Ö. Aydemir, "Olfaction recognition by EEG analysis using wavelet transform features". In IEEE International Symposium on Innovations in Intelligent Systems and Applications (INISTA), pp. 1-4, August 2016, doi: 10.1109/INISTA.2016.7571827.

[30] G. Mary, S. Chitti, R. B. Vallabhaneni, and N. Renuka, "EEG Signal Classification Automation using Novel Modified Random Forest Approach," *J. Sci. Ind. Res.*, vol. 82, no. 1, pp. 101–108, January 2023, doi: 10.56042/jsir.v82i1.70213.

[31] A. Sakalle, P. Tomar, H. Bhardwaj, D. Acharya, and A. Bhardwaj, "A LSTM based deep learning network for recognizing emotions using wireless brainwave driven system," *Expert Syst. Appl.*, vol. 173, no.1, p. 114516, July 2021, doi: 10.1016/j.eswa.2020.114516.

[32] S. Bagherzadeh, K. Maghooli, A. Shalbaf, and A. Maghsoudi, "Emotion recognition using continuous wavelet transform and ensemble of convolutional neural networks through transfer learning from electroencephalogram signal," *Front. Biomed. Technol.*, vol. 10, no. 1, pp. 47–56, January 2023, doi: 10.18502/fbt.v10i1.11512.

[33] Y. Luo, C. Wu, and C. Lv, "Cascaded Convolutional Recurrent Neural Networks for EEG Emotion Recognition Based on Temporal–Frequency–Spatial Features," *Appl. Sci.*, vol. 13, no. 11, p. 6761, June 2023, doi: 10.3390/app13116761.

[34] J. Kim, J. Oh, and T. Y. Heo, "Acoustic classification of mosquitoes using convolutional neural networks combined with activity circadian rhythm information," *Int. J. Interact. Multimedia Artif. Intell.*, vol. 7, no. 2, pp. 59-65, December 2021, doi: 10.9781/ijimai.2021.08.009.

[35] V. Gupta, M. D. Chopda, and R. B. Pachori, "Cross-subject emotion recognition using flexible analytic wavelet transform from EEG signals," *IEEE Sensors J.*, vol. 19, no. 6, pp. 2266–2274, March 2019, doi: 10.1109/JSEN.2018.2883497.

[36] H. Mei and X. Xu, "EEG-based emotion classification using convolutional neural network," *in* Proc. Int. Conf. Security, Pattern Anal., Cybern. (SPAC), Shenzhen, China, December 2017, pp. 130–135, doi: 10.1109/SPAC.2017.8304301.

[37] W. L. Zheng, J. Y. Zhu, and B. L. Lu, "Identifying stable patterns over time for emotion recognition from EEG," *IEEE Trans. Affect. Comput.*, vol. 10, no. 3, pp. 417–429, June 2017, doi: 10.1109/TAFFC.2017.2712143.

[38] M. Zangeneh Soroush, K. Maghooli, S. K. Setarehdan, and A. M. Nasrabadi, "A novel EEG-based approach to classify emotions through phase space dynamics," *Signal Image Video Process.*, vol. 13, pp. 1149–1156, March 2019, doi: 10.1007/s11760-019-01455-y.

[39] Y. H. Kwon, S. B. Shin, and S. D. Kim, "Electroencephalography based fusion two-dimensional (2D)-convolution neural networks (CNN) model for emotion recognition system," *Sensors*, vol. 18, no. 5, p. 1383, April 2018, doi: 10.3390/s18051383.